Synthesis and characterization of covalently grafted graphene oxide – poly (vinyl alcohol)/ carbon nanotubes nanocomposites

A. Rahim[a], K. Liaqat[a], S. Fazil[a], Z. Liaqat[b], S. A. H. Shah[c], W. Rehman[d,*],
M. Farooq[e], S. Haq[f], M. Nawaz[g]
[a]*Department of chemistry, University of Poonch Rawalakot, Azad Jammu and Kashmir, Pakistan*
[b]*Department of Physics, Abbottabad University of Science and Technology, Abbottabad, KP, Pakistan*
[c]*Department of Physic and chemistry, Universiti Tun Hussein Onn Malaysia.*
[d]*Department of Chemistry, Hazara University Mansehra. , KP, Pakistan*
[e]*Department of Physics, Hazara University Mansehra, KP, Pakistan*
[f]*Department of Chemistry, University of Azad Jammu & Kashmir, Muzaffarabad, Pakistan.*
[g]*Department of Chemistry, Balochistan University of Information Technology, Engineering and Management Sciences (BUITEMS), Airport Road Baleli, Quetta-87100, Pakistan*

Herein we have reported a simple procedure for the synthesis of covalently grafted graphene oxide poly (vinyl alcohol) (PVA-g-GO). Later on, multiwalled carbon nanotubes (MWCNTs) were dispersed in this PVA-g-GO matrix by sequential stirring and sonication. Nanocomposites with varying weight percent of graphene oxide (GO) and multiwalled carbon nanotubes (MWCNTs) were synthesized. These nanocomposites have shown excellent thermal and mechanical stability. It also appears that presence of graphene oxide has assisted in dispersing the MWCNTs. Combine effect of GO and MWCNTs has resulted in the nanocomposite with electrical conductivity of 2.02E-09 S/cm.

1. Introduction

In the last three decades, carbon nanomaterials have had an unparalleled influence on the scope and applications of nanotechnology. Beginning with the discovery of fullerenes and progressing through the carbon nanotube (CNT) era to graphene and other two-dimensional (2D) materials, the scientific world has been bombarded with innovative ideas, developments, and various attempts to find killer applications for this incredible nanostructure [1,2]. CNTs composites based on polymers, integration of these two types of components have resulted in improvement as well as emergence of unique properties. However, since CNTs have a clear propensity to accumulate, dispersion of CNTs in the polymer matrix for composite formulation is a challenging process, which becomes further complicated due to inert nature and lack of functional sites on CNTs surface [3, 4]. Various approaches can be adopted for preventing the aggregation of CNTs. One of them is covalently attaching various functional groups for improving dispersion and interconnection with matrix [5, 6]. The disruption of molecular structure of CNTs is associated with this approach and the properties of composites are therefore affected. Non-covalent functionality can be used for the dispersion of CNT into the polymer matrix as an alternative to covalent functionalization. Another approach uses polymer or surfactant for improving the dispersion of CNTs in a solvent and subsequently, for the formation of composite this mixture is then added in a polymer matrix. This second option is appealing as chemical structure of CNTs remains intact in it [7-10].

---

* Corresponding author: sono_waj@yahoo.com

Another carbon nanomaterial is graphene oxide, which is a two dimensional (2D) sheet of carbon atoms having variety of oxygen containing functional groups on its surface which results in its improved dispersibility [11,12]. Furthermore, recent researches have revealed that graphene oxide through noncovalent interaction can help to disperse CNTs in aqueous dispersion [13,14]. Mechanically graphene oxide is strong as compared to surfactant or polymer dispersants. Like CNTs, graphene oxide has also been incorporated into various polymers as reinforcement, and resulted in the improvement of mechanical properties [15-16]. Thus graphene oxide is expected to not only help in dispersing the CNTs in polymer matrix but a combination of graphene oxide and CNTs may reinforce the properties of polymer nanocomposites.

Present work support the synthesis of polymer nanocomposite for which graphene oxide was covalently grafted on the surface of poly (vinyl alcohol) and later on MWCNTs dispersion was added into it. We have synthesized the polymer nanocomposites with varying concentration of GO and MWCNTs while keeping the concentration of poly (vinyl alcohol) as constant. It is expected that this approach will help in fine dispersion of CNTs and combination of 1D and 2D will result in reinforcing mechanical as well as thermal stability of composites.

2. Experimental

2.1. Synthesis of graphene oxide

A two-step process was used for synthesizing graphene oxide. In the first step graphite oxide was prepared by modified Hummers's procedure in which 2.50 g of graphite and 5g of sodium nitrate (NaNO$_3$) were placed in cold concentrated H$_2$SO$_4$. While keeping the temperature of suspension fixed at 20°C, 7.5g of KMnO$_4$ was added into it. Mixture was then maintained at 35±3°C for 30 minutes. After that, deionized water was gradually poured in the mixture, resulting in the increase in temperature to 98°C. After 15 minutes, mixture was further diluted with deionized water and 5% hydrogen peroxide was added into it. After that, mixture was filtered and washed. Graphite oxide was obtained by drying the supernate.

The conversion of graphite oxide into graphene oxide was done by repetitive sonication and stirring in N, N-dimethylformamide (DMF)[17].

2.2. Synthesis of Synergic PVA-g-GO/MWCNTs Nanocomposite

Mixing of aqueous solution of PVA with GO dispersion in DMF was carried out and then a small amount of HCl was added to this mixture which was subjected to stirring. MWCNTs dispersion was added to this mixture was which was then stirred and ultrasonicated sequentially for overnight. Finally, PVA-g-GO/MWCNTs solution was casted onto petri dish and dried at 60°C. Nanocomposites with different loadings of GO and MWCNTs with respect to PVA was synthesized similarly. In addition PVA -g-GO and PVA /MWCNTs nanocomposite films were also synthesized for comparison.
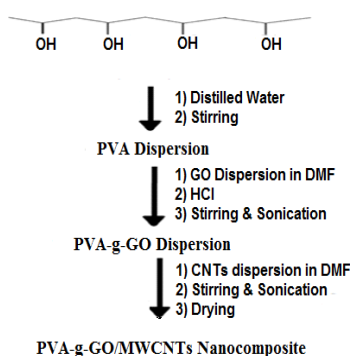

Fig. 1. Synthesis of PVA-GO-CNT Nano composite.

3. Characterization

3.1. FTIR Spectroscopy
PVA-g-GO/MWCNTs nanocomposites with various weight percentages were characterized with Thermo Scientific Nicolet 6700 in the range of 4000-500cm^{-1}

3.2. X-ray Diffraction
Rigaku D/A X-ray diffractometer was used for this characterization, Data was collected in the range of $2\theta=10^{o}$ to 50°

3.3. Thermogravimetric Analysis
NETZSCH TG 209 F1 instrument was used for determining the thermal stability of the nanocomposites with the heating rate of 10°C/min under nitrogen in the temperature range of 50°C to 700°C.

3.4. Mechanical Analysis
PVA-g-GO/MWCNTs nanocomposites were mechanically characterized with Instron 5565 electronic universal tensile strength at the rate of 2 mm/min. Results were recorded on average after testing five specimens for each sample.

3.5. UV-Vis Spectroscopy
UV−Vis absorption spectra of dispersed MWCNTs were recorded with a Shimadzu UV-3101PC spectrometer operating from 190 to 800 nm. For this purpose MWCNTs were taken after sonication and centrifugation at 3500 rpm for 15 min to remove the nondispersed nanotubes. Then, the supernatants were diluted by 100 times, resulting in the MWCNTs dispersions suitable for UV−Vis measurements.

3.6. Morphological Analysis
Scanning electron micrographs were acquired by using LEO 1530 VP field emission scanning electron microscope (FESEM).

3.7. Electrical Conductivity Measurement
PVA-g-GO/MWCNTs nanocomposites were analyzed by Impedance analyzer (ALPHA-A built by Novocontrol Technology) at room temperature.

4. Results and Discussions

4.1. Fourier Transform Infrared Spectroscopy
Even though intensities of the GO and PVA-GO spectra differ because of the esterification reaction, the FTIR spectrum (Fig. 2) of PVA-g- GO exhibits many bands present in the spectrum of GO. Notably, the peaks at 1022, 1091, and 1261 cm^{-1} correspond to the stretching modes of the C–O group of the ester while the peak at 1750 cm^{-1} in the spectrum of PVA-g-GO is attributed to the C=O stretching of newly formed carbonyl groups on the surface of the GO, indicating existence of covalently bonded PVA chains on surface of GO. Meta distribution process undergone in most of benzene rings of CNTs was indicated by peaks in the region of 750–840 cm^{-1} and 840–900 cm^{-1} [18].
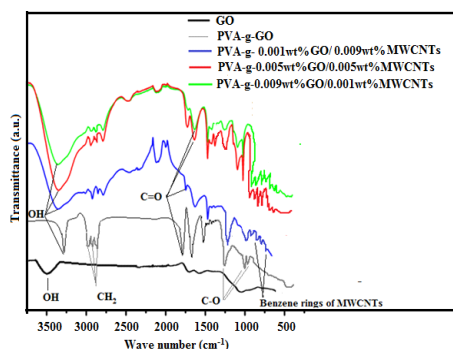
Fig. 2. FTIR spectra of pure GO, PVA-g-GO and PVA-g-GO/MWCNTs with
varying concentrations of GO and MWCNTs.

4.2. X-Ray Diffraction Analysis

Diffraction peak of PVA appears at 20°, correspond to 101 plane demonstrating its semi-crystalline structure [19, 20], whereas PVA-g-GO diffraction peak appears at $2\theta = 25^o$. Pure MWCNTs shows two diffraction peaks at 26.10^o and 43°, corresponding to 002 and 100 planes of the graphitic structure of MWCNTs [22]. In the diffraction pattern of PVA-g-GO/MWCNTs, a single peak appears at $2\theta = 25^o$. Diffraction peaks due to MWCNTs does not appear in pattern of diffraction PVA-g-GO/MWCNTs indicating the homogeneous dispersion of MWCNTs in PVA-g-GO matrix. Intensity of composite's peak increases along with increase in contents of GO (Fig. 3).
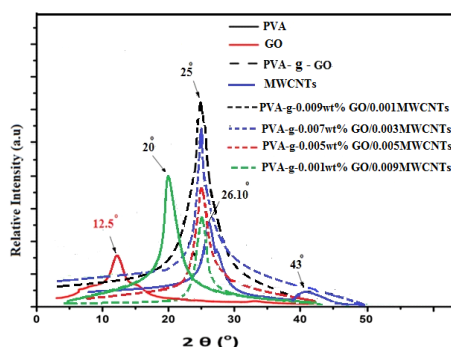

Fig. 3. X-ray diffraction analysis of PVA, GO, GO-g-PVA, MWCNTs, GO-g-
PVA/MWCNTs with varying concentrations of GO and MWCNTs.

4.3. Thermogravimetric Analysis

Thermal stability of synthesized nanocomposites was analyzed in temperature range of 50-700°C at a heating rate of 10 °C/min, in the presence of nitrogen and results are presented in the Fig. 4. Initial weight loss in the thermal gravimetric analysis of GO is attributed to the decomposition of an oxygenated functional group. Whereas, in the case of the GO-g-PVA, this initial weight loss is shifted to high temperature, which might be due to esterification reaction used to graft PVA to GO that result in the loss of some of oxygen-containing functional groups. Majority of PVA decomposes from 250 to 350 °C, with the residual weight reaching to about 10 wt% at 700 °C. Residual weight for GO at 700 °C is about 42.5 %, while that of GO-g-PVA is 27.5 wt%, indicating the increase in thermal stability of GO grafted PVA. From this Figure it appears that as the GO/MWCNTs concentration varies from 0.001wt% GO / 0.009 wt% MWCNTs to 0.009 wt % GO/ 0.001g MWCNTs, residual weight %age decrease from 50 to 35%. It appears that this increase in thermal stability is not only because of grafting of GO on the surface of PVA, but also due to the presence of MWCNTs.
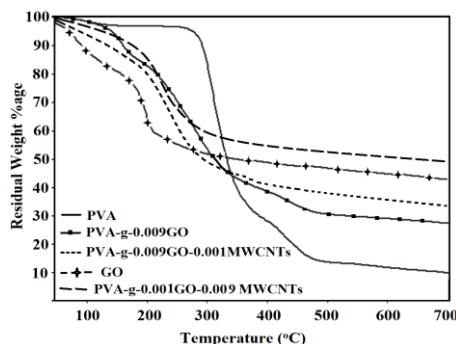
Fig. 4. Thermogravimetric analysis of GO, PVA-g-GO and PVA-g-GO/MWCNTs with varying concentrations of GO and MWCNTs.

4.4. UV-Vis spectroscopic Analysis

UV- Vis spectroscopy was used for quantitative assessing the effectiveness of PVA-g- GO /MWCNT in exfoliating MWCNTs. Wrapped MWCNTs are inactive in wavelength range between 200 to 1200 nm whereas individual MWCNTs are active and their absorption increases with their exfoliation. UV-vis absorption spectra can be used for determining dispersion of both MWCNTs [22,23] and SWCNTs[24,25]. Beer-Lambert law was used for establishing a relation between the concentrations of suspended MWCNTs and their absorbance (eq 1)

$$A = \varepsilon c l \qquad (1)$$

Here absorbance at particular wavelength (261nm) is represented by "A", extinction coefficient is represented by "ε", path length of cell is "l" and concentration is given by "c". The weight of PVA-g-GO was subtracted from dry weight of supernatants in order to estimate the concentrations of MWCNTs in supernatants.

Fig. 5a represents UV-Vis spectrum of PVA-g-GO /MWCNTs with different MWCNTs concentration and a fixed PVA-g-GO /MWCNTs mass ratio of 1:1. Slope calculated by applying least square fitting is 150 and therefore 'ε' (molar attenuation coefficient) of MWCNTs is 150 mL mg^{-1} cm^{-1} (Fig. 5b). Exact concentration of dispersed MWCNTs in solution can be obtained from molar attenuation coefficient 'ε' and absorbance data. In order to check the effectiveness of graphene oxide in dispersing MWCNTs, different weight percent of graphene oxide was covalently attached to the surface of PVA (fixed weight) later on MWCNTs were dispersed into PVA-g-GO dispersion. As UV absorbance is only because of MWCNTs, therefore by using 'ε' and absorbance data we easily find the exact concentration of dispersed MWCNTs. For this particular study we have selected 0.005mg/mL concentration of MWCNTs and varying concentration of graphene oxide (0.010 to 0.001mg/mL) were used. Results are presented in the form of Figure 4c which indicates that when ratio of dispersant to MWCNTs is 2:1 than the dispersed concentration of MWCNTs reaches to 0.0047. Ionizable carboxyl groups present on edges of graphene oxide make it soluble in water. The immoderate adherence of MWCNTs to graphene oxide sheets results in their aggregation on GO sheets causing failure of maintaining dispersion stability in water. While partially hydrophobic graphene oxide basal planes cause restriction in binding of whole quantity of MWCNTs on graphene oxide sheets. Liu *et al*.,[13] studied dispersion of MWCNTs in aqueous media which was assisted by GO and he came to know that excess of MWCNTs on graphene oxide sheets may decrease the solubility of the GO/MWCNT composite and it leads to a degree of agglomeration when GO to MWCNT weight ratio is 0.5 : 1. A well stable dispersion is achieved with ratio 2:1 or higher.
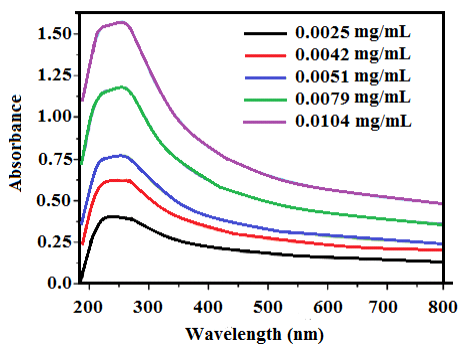
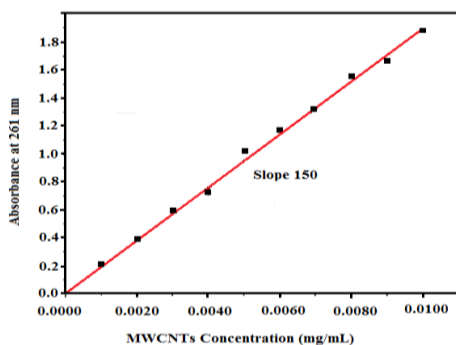*Fig. 4a. Absorbance plotted against wavelength for PVA-g-GO /MWCNTs solutions.*

Fig. 5b. UV−Vis absorption spectra of PVA-g-GO /MWCNTs solutions with different MWCNTs concentrations.
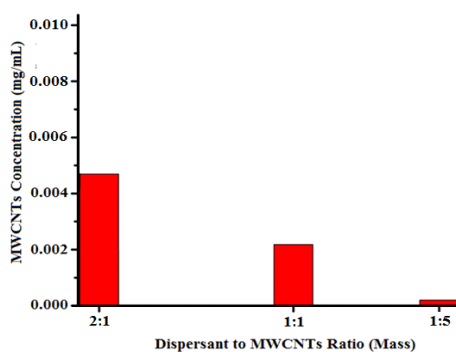

Fig. 5. c Effect of various concentration of GO on dispersing the MWCNTs.

4.5. Morphological Analysis

Morphology of nanocomposites as well as polymer is confirmed by SEM. Surface of pristine polymer is smooth (Fig. 6a). In case of PVA/MWCNTs there are aggregates of MWCNTs (Fig. 6b). Surface of PVA-g-GO nanocomposite is rough as compared to polymer (Fig. 6c). MWCNTs dispersion becomes homogeneous in the presence of Go as appears from the Fig. 6d.
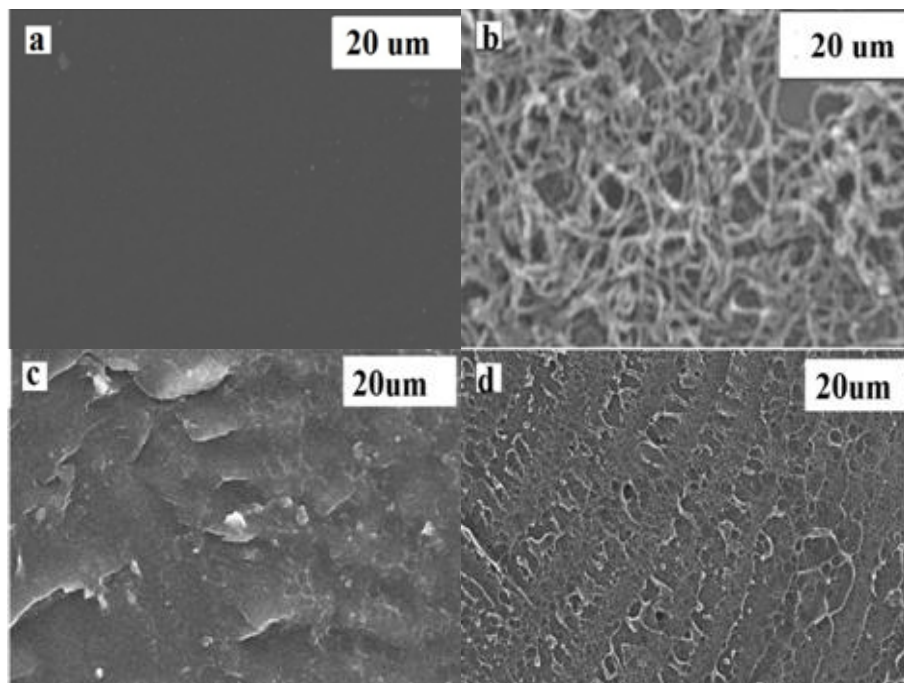
*Fig. 6. SEM images of a) PVA b) PVA/0.01 wt% MWCNTs c) PVA-g-0.01 wt% GO
d) PVA-g-0.005 wt% GO/ 0.005 wt% MWCNTs.*

4.6. Mechanical Analysis

For studying the combine effect of graphene oxide and multiwall carbon nanotubes on the mechanical properties of PVA-g-GO /MWCNTs nanocomposites, we have compared the mechanical properties of films containing various loading of graphene oxide and MWCNTs with those of PVA-g-GO and PVA/MWCNTs nanocomposite films. All the results are summarized in Table 1. From this Table, it appears that with addition of 0.010 wt% pristine MWCNTs, tensile strength and Young's modulus increase by 4.85% and 2.61% whereas elongation at break decreases by 6.71% respectively. In contrast, with the grafting of 0.010 wt% GO on PVA (PVA-g-0.010 wt% GO), tensile strength and Young's modulus increases by 41.24% and 22.58% respectively, while elongation at break decreases by 1.49%. Despite uniform and homogeneous dispersion of MWCNTs their reinforcement effect is low which might be due to their inert surface, resulting in weak interfacial adhesion between them and matrix. On the other hand GO due to its hydrophilic nature acts as good reinforcing agent [26]. At last, it is found that combined effect of grafted GO and MWCNTs to mechanically reinforce the matrix is superior as compared to that of single component filler. With the decrease in the weight content of g-GO 0.09 to 0.001 wt% and corresponding increase in the weight content of MWCNTs from 0.001 to 0.09 wt%, tensile strength increases from 66.5 MPa to 88.5 MPa after which it decreases to 78 MPa, elongation at break increases from 49.7% to 59.5% and young's modulus increases by 59% respectively. This reinforcement is due to combined effect of graphene oxide and MWCNTs and is quite high as compared to reinforcing effect of the individual filler.

Table 1. Mechanical Properties of Nanocomposites.

Sample Type	Composition (wt%)		Tensile Strength (MPa)	Elongation at Break (%)	Young's Modulus (GPA)
	GO	MWCNTs			
1	0	0	57.7	53.7	3.1
2	0.01	0	81.5	52.9	3.8
3	0.009	0.001	66.5	49.7	3.9
3	0.008	0.002	73.7	50.2	4.4
4	0.007	0.003	78.7	51.5	4.8
5	0.006	0.004	84	52.1	5.2
6	0.005	0.005	86.5	53.5	5.4
8	0.004	0.006	87.5	55.5	5.6
9	0.003	0.007	88.5	56.5	5.8
10	0.002	0.008	82.5	58.0	6
11	0.001	0.009	78	59.5	6.2
12	0	0.01	60.5	50.1	3.3

4.6. Electrical Conductivity Analysis

Fig. 7 exhibits the changes in electrical conductivity of PVA-g-GO/MWCNTs nanocomposites with varying concentrations of GO and MWCNTs. Electrical conductivity of PVA at 298K is 1.63 E-12 S/cm. In case of nanocomposite (PVA-g-GO/MWCNTs) electrical conductivity gradually increases as the concentration of MWCNTs increases and achieves maximum value at 0.005 wt% of GO/MWCNTs after that it decreases. This increase in electrical conductivity of nanocomposite might be due to the presence of MWCNTs which are electrically conductive. It is expected that the foreign entities (GO& MWCNTs) will form interfaces with the polymer matrix (PVA). These interfaces are usually electrically active which generate holes, ions and electrons. In PVA-g-GO/MWCNTs system, ions such as H+ and COO− can interact also resulting a charged surface that is linked with the local electric field. The conduction of ions and conductivity is increased due to this space charge-induced enhancement effect. More addition of filler content enhances the number density of mobile ions, which results in formation of conductivity chain. [27–29].
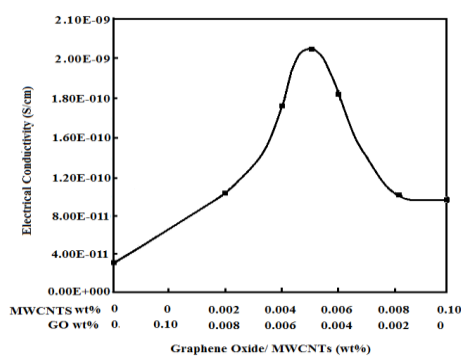

Fig. 7. Electrical conductivity analysis of PVA-g-GO/MWCNTs composites with varying concentrations of GO and MWCNTs.

5. Conclusion

We have developed an easy procedure to synthesize graphene oxide (GO) functionalized poly (vinyl alcohol) (PVA)/MWCNTs nanocomposites with varying concentration of graphene oxide and MWCNTs. Synthesized PVA-g-GO composites were subjected to FTIR, XRD, TGA and SEM characterizations for analysis of morphology and chemical structure. PVA-g-GO has better ability to make MWCNTs dispersed and stable in DMF solutions via noncovalent interactions. The efficiency of PVA-g-GO to disperse MWCNTs is quantitatively assessed by UV-visible spectroscopy. With the weight ratio of PVA-g-GO to MWCNTs (2:1) and initial

concentration of MWCNTs 0.005 mg/mL, the dispersed concentration of MWCNTs achieved a value of 0.47 mg/mL, which is significantly greater. Subsequently, effect of various concentration of GO, MWCNTs, g-GO and g-GO / MWCNTs were compared in enhancing the mechanical properties of nanocomposites. It was found that GO and MWCNTs together have performed better than the single fillers in the reinforcement of PVA. Combined effect of GO and MWCNTs has resulted in the 43% increase in tensile strength, 10% increase in elongation at break and 100% increase in Young's modulus respectively. PVA shows the electrical conductivity of 1.63×10^{-12} S/cm at 298K whereas electrical conductivity of PVA-g-GO/MWCNTs nanocomposites reached to 2.02E-09 S/cm which might be due to the formation of charged specie.

References

[1] J. N. Coleman, U. Khan, W. J. Blau, Y. K. Gunko, Carbon **44**, 1624 (2006).
[2] A. L. Ma-Hernandez, C. Ve-Santos, V. M. Castano, Curr. Nanosci. **6**, 12 (2010).
[3] M. Moniruzzaman, K. I. Winey. Macromolecules **39**, 519 (2006).
[4] B. P. Grady, Macromol, Rapid Commun. **31**, 247(2010).
[5] X. L. Xie, Y. W. Mai, X. P. Zhou. Mater. Sci. Eng. R Rep. **49**, 89 (2005).
[6] N. G. Sahoo, S. Rana, J. W. Cho, L. Li , S. H. Chan. Prog. Polym. Sci. **35**, 837(2010).
[7] J. Q. Liu, T. Xiao, K. Liao, P. Wu. Nanotechnology **18**, 165701 (2007).
[8] X. H. Peng, S. S. Wong, Adv. Mater. **21**, 625 (2009).
[9] H. Wang. Curr. Opin. Colloid Interface Sci. **14**, 364 (2009).
[10] C. Y. Hu, Y. J. Xu, S. W. Duo, R. F. Zhang, M. S. Li. J Chin. Chem. Soc. **56**, 234 (2009).
[11] O. C. Compton, S. T. Nguyen. Small **6**, 711 (2010).
[12] D. R. Dreyer, S. Park, C. W. Bielawski, R. S. Ruoff. Chem. Soc. Rev. **39**, 228 (2010).
[13] C. Zhang, L. L. Ren, X. Y. Wang, T. X. Liu. J. Phys. Chem. C **114**, 11435 (2010).
[14] C. G. Navarro, M. Burghard, K. Kern. Nano Lett. **8**, 2045 (2008).
[15] H. Jin, C. Guo, X. Liu, J. Liu, A. Vasileff, Y. Jiao, Y. Zheng, S. Z. Qiao. Chem. Rev. **118**, 6337   (2018)
[16] P. Liu, Z. Yao, J. Zhou, Polym. Compos. **38**, 2321 (2017).
[17] W. S. Hummers, R. E. Offeman, J. Am. Chem. Soc. **80**, 1339 (1958).
[18] E. Y. Malikov, M. B. Muradov, O. H. Akperov, G. M. Eyvazova, R. Puskás, D. Madarász, L. Nagy, Á. Kukovecz, Z. Kónya. Physica E **61**, 129 (2014).
[19] N. S. Alghunaim, Result phys. **6**, 456 (2016).
[20] A. Abdolmaleki, S. Mallakpour, F. Azimi. Eur. Polym. J. **87**, 277(2017).
[21] Y. J. V Ruban, S. G. Mon, D. V. Roy. Int. J. Plast. Technol. **15**, 133 (2011).
[22] J. R. Yu, K. B.Lu, E. Sourty, N. Grossiord, C. E. Konine, J. C. Loos, **45**, 2897 (2007).
[23] J. Rausch, R. C. Zhuang, E. Mader. Composites Part A **41**, 1038 (2010).
[24] W. Yuan, J. L. Feng, Z. Judeh, J. Dai, M. B. C-Park. Chem. Mater. **22**, 6542 (2010).
[25] N. Grossiord, O. Regev, J. Loos, J. Meuldijk, C. E. Koning. Anal. Chem. **77**, 5135 (2005).
[26] Y. Pan, T. Wu, H. Bao, L. Li. Carbohydr. Polym. **83**, 1908 (2011).
[27] R. C. Agarwal, R. K. Gupta. J. Mater. Sci. **34**, 1131 (1999).
[28] A. Mikkrajuddin, F. G. Shi, K. Okuyama. J. Electrochem. Soc. 147, 3157 (2000).
[29] P. Knauth, J. Electroceram. **5**, 111 (2000).